Modelling heterogeneous photocatalytic oxidation using suspended TiO 2 in a photoreactor working in continuous mode: Application to dynamic irradiation conditions simulating typical days in July and February

Gaël Plantard, Chloé Dezani, Enrique Ribeiro, Brice Reoyo-prats, Vincent Goetz

Modelling heterogeneous photocatalytic oxidation using suspended TiO_2 in a photoreactor working in continuous mode: application to dynamic irradiation conditions simulating typical days of July and February.

Gael PLANTARD [(1),(2)], Chloé DEZANI [(1),(2)], Enrique RIBEIRO[(1),(2)], Brice REOYO-PRATS[(1),(2)], Vincent GOETZ [(1)]

[(1)] PROMES CNRS, UPR 8521, Rambla de la thermodynamique 66100 Perpignan, France.
[(2)] University of Perpignan Via Domitia, 52 Paul Alduy 66100 Perpignan, France.

Email address: plantard@univ-perp.fr

ABSTRACT

Compared to more conventional techniques, advanced oxidation processes (AOP) hold huge promise in terms of elimination of organic (especially 'persistent') compounds and microorganisms (disinfection) in wastewater. If the objective is to power these processes using solar energy, we need to be able to manage the intermittency in the solar resource. This is an essential step for design and to ensure efficient operation of the treatment processes. As solar radiation is inherently variable due to day/night cycles, seasonal cycles, and weather meteorological conditions, solar AOP performances are difficult to establish using conventional measures. To address this gap, we carry out experimental campaigns under controlled conditions and develop modeling tools capable of describing dynamic-mode photocatalytic degradation. Here we develop a way to capture the responses of a photoreactor subjected to various stresses, including irradiation conditions, via an LED panel. Using a model that considers the influence of UV flux density and pollutant concentration made it was possible to represent photoreactor responses under different irradiation conditions and feeds (concentration or flow at the input). The ultimate objective is to study the photocatalytic capacity of the photoreactor under irradiation conditions simulating a real day of sunshine.

GLOSSARY

CSTR	*Continuous stirred-tank reactor*
LED	*Light-emitting diode*
LH	*Langmuir Hinshelwood*
MO	*Methyl orange*
PMMA	*Poly(methyl methacrylate)*
UV	*Ultra violet*

SYMBOL

I	*incident flux density*	$W.m^{-2}$
q_e	*adsorption capacity at equilibrium*	$kg.kg^{-1}$
q_m	*maximum monolayer adsorption capacity*	$kg{\cdot}kg^{-1}$
C_e	*the equilibrium concentration*	$kg.m^{-3}$
b	*the constant related to energy of adsorption*	$m^3.kg^{-1}$
m_v	*the flow rate*	$m^3.s^{-1}$
C_i	*the concentration at the inlet of the reactor*	$kg.m^{-3}$
C_0	*the concentration at the outlet of the reactor*	$kg.m^{-3}$
V_r	*the volume of the photoreactor*	m^{-3}
V_T	*the volume of the system including the loop and reactor*	m^{-3}
$\overset{\circ}{r}$	*photoreaction rate*	$kg.m^{-3}.s^{-1}$
α	*constant of the photoreaction*	$m^2.J^{-1}$
β	*parameter modulating reaction rate with respect to concentration*	$m^3.kg^{-1}$
γ	*parameter modulating reaction rate with respect to irradiation*	$m^2.W^{-1}$
τ	*the residence time*	s
τ_{irr}	*the irradiation time*	s
k	*the number of experimental data*	*(-)*
C_{cal}	*the calculated concentration*	$kg.m^{-3}$
C_{exp}	*the experimental concentration*	$kg.m^{-3}$

1. INTRODUCTION

It is now well established that organic compounds are a significant source of pollution and a very high risk to human health[1-3]. To overcome the shortcomings of biodegradation-based processes, a number of innovative technologies[4-14] have been developed to eliminate biorecalcitrant organic pollutants, microorganisms, and more. In this context, compared to so-called tertiary treatment techniques, advanced oxidation processes (AOPs) hold huge promise and are particularly effective at removing persistent organic compounds in wastewater. Membrane and adsorption processes can offer technical solutions to fix pollutants but not to degrade them,[15-16] whereas photo-oxidation presents three significant advantages: low-temperature operation, no chemical additives, and—crucially—the possibility to use solar energy to activate the photochemical process[17]. In heterogeneous photocatalysis based on the use of radiation, the highly oxidizing species are produced by a solid photocatalyst under UV irradiation. As a result, when combined with direct use of solar power,[9] this process is almost energy-self-sufficient and makes it possible to design a water treatment process that is simple, robust and inexpensive to install and operate[10-13]. In 2002, on the PSA site[10] researchers conducted pilot-scale experimental campaigns using solar energy. Using an experimental approach, they described pilot-scale wastewater treatment technologies and the allied parameters based on photochemical reactions. More recent research[18] shows that one of the major problems encountered in the field of AOPs is the use of sunlight. Indeed, if the objective is to use solar resources, we need to consider two specific features of solar radiation. First, sunlight is particularly weak in the UV spectral region, unlike lamps that provide an intense and constant beam of light. The UV spectral region represents only 5% of total solar flux available at the Earth's surface,[19] which represents a maximum available irradiation of 50 $W_{UV}.m^{-2}$. The second constraint to consider for efficient design and use of a photoreactor is the intermittency of sunlight. Radiation variations during day-night and seasonal cycles[20-22] make it a complex task to select the right operating conditions and predict how the photochemical process will perform. Thus, to scale-up a solar oxidation process, it become essential to model the capacity of a photoreactor operating under dynamic conditions, both from the irradiation side and the supply conditions side. The vast amount of research carried out on pollutant degradation processes is almost entirely based on photoreactors operating in batch mode,[23-24] which makes it difficult to translate results into real-world-based processing operations which inevitably operate in a pseudo-continuous mode. Thus, in order to design solar-based photooxidation processes, it is necessary to conduct experimental campaigns in

'dynamic' conditions (typically irradiation and flow rate) and to develop modelling tools that describe photoreactor capacity in continuous-mode operation.

Here we developed a photochemical process capable of operating in continuous mode. This process consists of a photoreactor fed by single passage of pollutants. This photoreactor can operate under a flux density simulating solar irradiation conditions but also with variable pollutant concentrations and flowrates. The experimental set-up equipped with an LED panel makes it possible to apply firmly-controlled irradiation setpoints. Thus, unlike UV incandescent lamps whose flux density cannot be precisely fixed or modulated at small timesteps, LEDs can produce variable flux densities as well as daylighting setpoint of a typical day. Experimental tests were performed in different operating conditions—flow rate, flux density, and concentration—to study the influence of these variables. Modelling the capacities of the photoreactor made it possible to simulate the pilot's responses, as well as providing sizing tools for the design and scaling of solar reactors operating in dynamic mode. This model,[25-26] which depends on flux density and pollutant concentration level, is primarily designed to account for the discontinuous nature of solar irradiation. We selected a target substance to perform the experiments under perfectly controlled conditions, and we used a database to propose, validate and test the model taking into account material balance in the photoreactor. Here we focus on aspects of process engineering with a photoreactor operating in dynamic mode, which have insufficiently addressed in the literature. The ultimate aim of this research was to assess the photocatalytic capacity of a photoreactor process using LEDs to apply irradiation simulating a day of sunshine.

2. MATERIALS AND METHODS

2.1. Catalyst, target substances and analytical tools

The photocatalyst was TiO_2, the material most widely used for this purpose. In this study, P-25 was taken as the reference material on account of its photocatalytic behaviour. Its specific surface area (BET) was 54 $m^2.g^{-1}$ and the particles of TiO_2[9-10, 25, 27] had an average diameter of about 20 nm. In a previous publication,[5] we correlated catalyst concentration with transmittance capacity to optimize catalyst design for different reactor geometries. In this study, a concentration of 0.2 $g.L^{-1}$ was needed to absorb the total incident radiation at the surface of the photoreactor.

Methyl orange (MO) was chosen as an indicator to follow the effect of operating conditions. To determine the change in the methyl orange concentration after MO removal during UV irradiation, samples of the suspension were withdrawn regularly from the reactor,

and suspended solid matter removed with a syringe filter (pore size 0.45 µm). The clean transparent solution was analyzed by UV-Vis spectroscopy (Thermo scientific Evolution 600 spectrophotometer) after filtration. The MO concentration was measured from the absorbance at 480 nm using a calibration curve. Repeat tests were done to ensure reproducibility. For kinetic analyzis, each sample taken from the reactor was divided into three different vials, and the final absorption was taken as the arithmetic average over the three measurements.

2.2. Experimental set-up

The photochemical process is in a flat-type configuration illustrated in Figure 1,[20] essentially consisting of a photoreactor irradiated by an LED panel.

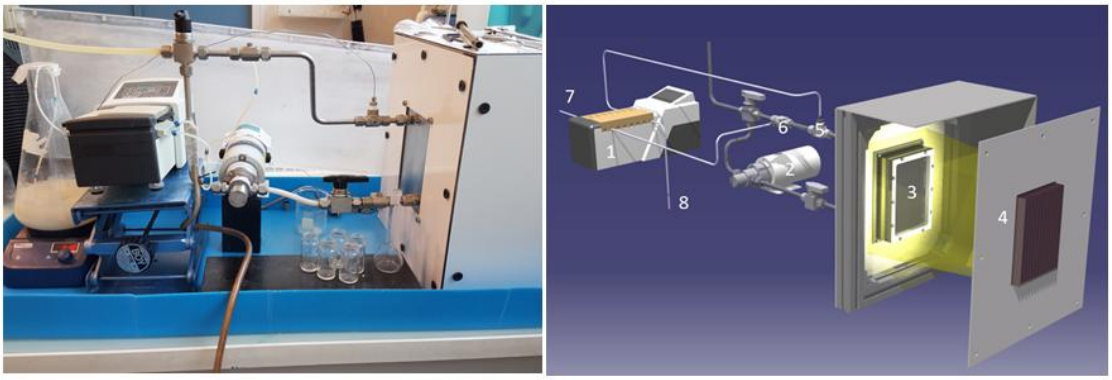

Figure 1 : Scheme and picture of the processing loop: peristatic pump (1), centrifugal pump (2), photoreactor (3), UV panel (4), withdrawal valve (5), feed valve (6), effluent at the inlet of the reactor (7), and effluent at the outlet of the reactor.

It operates as a perfectly stirred reactor fed in continuous mode with controlled flow and irradiance conditions. It has three parts: a photoreactor connected to a recirculation system, an LED panel as light source, and a micropump system to feed the loops. The photoreactor itself consists of a 0.1 m-wide, 0.15 m-long, 0.01 m-thick parallelepipedal window (3). A transparent PMMA plate transmits 95% of the LED-generated radiation (4). Distilled water used for all experiments is circulated using a variable speed centrifugal pump (2) (Cole-Palmer Instruments) to feed the photoreactor from bottom to top. This feed mode makes it possible to obtain a homogeneous concentration of particles in the solution. Total loop volume was 0.00025 m^3. The LED panel consists of 280 LEDs arranged in 10 rows generating UV radiation. The spectral field centred on a 375 nm is spread on 360-400 nm wavelength [28, 29]. The whole irradiation system is placed in a closed chamber to isolate it from any external light source. The parallelepiped window coupled to the LED panel corresponds to an irradiated surface per unit volume of 10^{-4} $m^2.m^{-3}$. The system can provide a UV radiation flux density in the range 1 to 170 $W.m^{-2}$ at an accuracy of 0.2 $W.m^{-2}$. This range of UV flux density corresponds to that of three suns. Irradiation conditions can be controlled

using a software interface, which makes it possible to apply flux density homogeneously over the entire range of available radiation and to simulate the solar radiation of a typical day, e.g. in February or July, in sunny or cloudy weather, in seasonal cycles or daily cycles, etc. The third part corresponds to the feed system and homogenization of the solution at the inlet of the photoreactor. It essentially consists of a multi-channel peristaltic pump (1) (Watson-Marlow 205CA) to maintain the continuous flow regime. The pump is connected to a storage tank and to the inlet of the loop (7). The photoreactor is fed with a solution consisting of a suspension of catalyst and MO at a given concentration. The photoreactor output (5) is also connected to the micropump to simultaneously empty the volume of solution corresponding to the one entering at the inlet of the photoreactor. In this configuration, range of flow can be made to vary between 0.016 and 0.16 ($.10^{-6}$) $.m^3.s^{-1}$, thus maintaining a fixed volume of fluid in the system.

3. PRELIMINARY RESULTS

3.1. Isotherm capacity

Adsorption equilibrium experiments were performed under dark conditions. A stock solution of 1 $kg.m^{-3}$ of pollutant was prepared by dissolving 0.001 kg of analytical reagent in 0.001 m^3 of distilled water. The adsorption isotherms were derived from measurements carried out in magnetically-stirred beakers (0.00025 m^3) each containing 0.0001 m^3. The tests were carried out at several initial MO concentrations in the range 0.01–0.5 $kg.m^{-3}$ while maintaining a constant catalyst concentration (1 $kg.m^{-3}$). Once equilibrium is reached, the quantity of MO adsorbed (q_e) is deduced from the experimental data. The time required to reach the adsorption equilibrium was estimated based on a previous study[30].

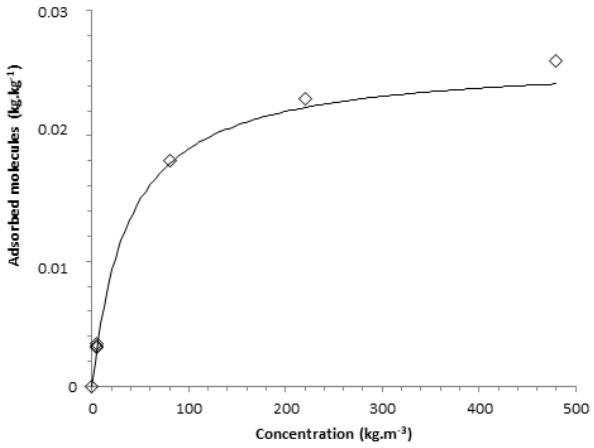

Figure 2 : Experimental isotherm obtained with MO in tap water at 25°C in a suspension of nanoparticles of titanium dioxide (◊). Results are fitted with LH (-).

Figure 2 shows the MO adsorption isotherm on the catalyst slurry, where q_e is plotted against C_e, the concentration of MO remaining in the solution once equilibrium is reached. In agreement with the literature,[25] the catalyst has a low adsorption capacity, mainly due to its non-microporous texture. The adsorption equilibrium isotherms were modelled using the Langmuir isotherm. Langmuir's theory,[31] based on the hypothesis of monolayer adsorption occurring on a homogeneous surface, is represented by the following equation:

$$q_e = q_m \frac{bC_e}{1+bC_e} \quad (1)$$

where q_e is the adsorption capacity at equilibrium (kg.kg^{-1}), q_m is the maximum monolayer adsorption capacity (kg·kg^{-1}), C_e is the equilibrium concentration (kg.m^{-3}), and b is a constant related to energy of adsorption (m^3.kg^{-1}). The Langmuir fittings were performed with q_m = 0.25 kg.kg^{-1} and b = 25 m^3.kg^{-1}. Experimental results and identification of q_m showed that whatever the initial concentration of pollutant, a negligible quantity of MO was adsorbed. Due to the low adsorption capacities of MO/TiO_2, the mass transfer could be neglected in degradation kinetic equations.

3.2. Continuous stirred tank photoreactor

To conduct the experiments, the photoreactor has to operate as a continuously-fed stirred-tank reactor. The characteristics of the processing loop, and in particular the residence time of the system, were therefore defined. Experimental residence time was determined taking into account photoreactor and circuit volume. The experimental data, i.e. the inlet and outlet

concentrations of the photoreactor, were acquired under different operating conditions. Different input concentrations were applied to assess the homogeneity of the system (Figure 3): the entire treatment loop was fed with MO solutions at concentrations of 0.2, 0.1, 0.02 and 0.01 kg.m^{-3}, but at a fixed rate.

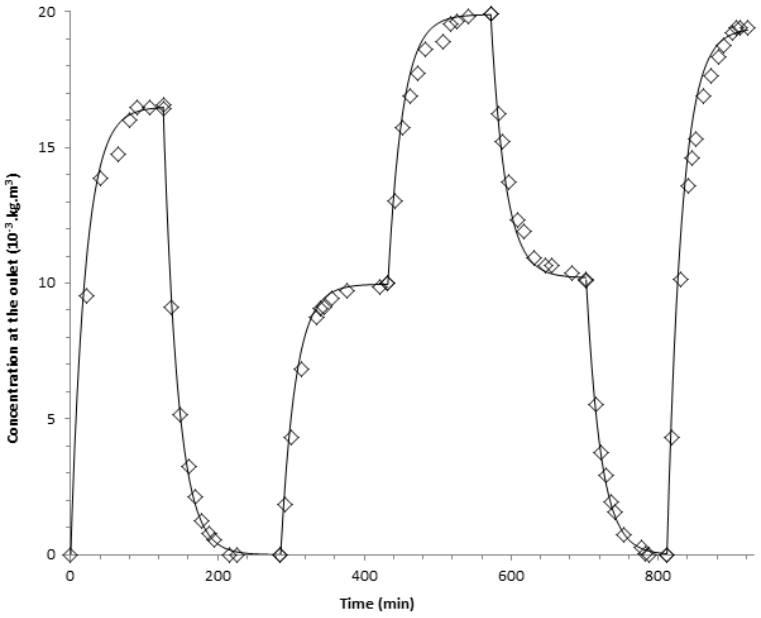

Figure 3 : Evolution of the concentration at the oulet of the photoreactor (◊) when applying different concentration at the inlet : 0.2, 0.1, 0.02, and 0.01 kg.m^{-3}. Results are fitted with Eq. 3.

To describe the concentration variations in the photoreactor, we established the material balance including the inlet and outlet conditions and a term expressing photodegradation. In Equation (2), the variation of the pollutant concentration in the photoreactor is described assuming that sorption phenomena at the catalyst surface are negligible [20, 24-25].

$$m_v C_i = m_v C_O(t) + V_r \overset{\circ}{r}(C, I, t) + V_T \frac{dC_o(t)}{dt} \qquad (2)$$

where m_v is the flow rate (m^3.s^{-1}), C_i is the inlet concentration (kg.m^{-3}), C_o is the outlet concentration (kg.m^{-3}), V_r is the irradiated volume (m^{-3}), V_T is the total volume of the loop (m^{-3}), $\overset{\circ}{r}$ is the speed of the photoreaction (kg.m^{-3}.s^{-1}) and $\frac{dC_o(t)}{dt}$ is the term for matter accumulation corresponding to the transient regime.

If the photoreactor is in the dark, the photo degradation term becomes zero. Thus the concentration in the reactor depends only on the input conditions, i.e. the concentration and the flow rate applied. The variation in the concentration is described by Equation (3).

$$C_o(t) = C_i(t) - (C_i(t) - C_{i0})e^{\frac{-t}{\tau}} \quad (3)$$

where $\frac{V_T}{m_v} = \tau$ is the average time a volume element of fluid stays in the system (called residence time) (s^{-1}), C_{i0} is the initial input concentration applied to the photoreactor, and $C_i(t)$ is the stepped input concentration applied to the photoreactor. Theoretical concentrations from the resolution of Equation (3), taking into account the operating conditions (inlet and outlet concentration, volume of the system and flow rate) are also reported in Figure 3. The residence time τ was found with an optimization method using a trust-region-reflective algorithm[24]. The profiles of the calculated pollutant concentrations at the outlet of the processing loop were plotted against time. The curves of calculated and measured concentrations coincided, indicating that the processing loop operated as a CSTR. The calculated residence time was 0.67 h. The difference between the calculated and the experimental results gave a dead volume of less than 2% of the total volume, which was considered negligible in the rest of the study. This result validates the fact that the photoreactor can be assimilated to a perfectly agitated reactor.

4. EXPERIMENTAL RESULTS

To highlight the importance of the operating conditions, a series of experiments were conducted at different flux densities, flow rates and feed concentration. We aimed to quantify the effects of the key variables on the capacity of the photoreactor to degrade a target pollutant. The performance of the process is defined by the rate of photoreaction resulting from the matter balance in Equation (2).

4.1.Flux density effect

Given the inevitable variability in the levels of irradiation during solar experiments, knowing the influence of the UV flux density on the kinetics is necessary to simulate the concentration profile as a function of time. In the laboratory set-up, photodegradation was investigated under different UV radiation fluxes, in the range 1–170 W m^{-2}, corresponding to flux from 0 to 3 suns (incident on the earth's surface). This set of experiments was carried out with fixed operating conditions, namely a concentration of MO of 0.02 $kg.m^{-3}$ and a flow rate of $0.08.10^{-6}$ $m^3.s^{-1}$ applied at the input of the reactor. The photoreactor window was irradiated at a flux density of 170 W m^{-2}, thereby engaging the photoreaction. The concentration in the system decreased until an equilibrium concentration was reached. Operating in an open

reactor, the threshold corresponded to the steady state of the system for which the accumulation term was zero. Thus once this phase occurred, the rate of degradation was deduced directly from Equation (4).

$$\frac{m_v}{V_r}(C_i - C_o(t)) = \overset{\circ}{r}(C, I, t) \quad (4)$$

where $\frac{V_r}{m_v} = \tau_{irr}$ is the average time of irradiation of a volume of fluid (called irradiation time) (s).

The next experiment was conducting directly after the first one, changing the applied flux density to 100 W m^{-2} and maintaining the concentration at 0.02 $kg.m^{-3}$ and the flux rate at 0.08 $.10^{-6}$ $m^3.s^{-1}$. The concentration thus decreased until a new equilibrium was reached, corresponding to the steady state of these new conditions (lower flux density). In the same way, new flux densities were applied successively. Results are reported in Figure 4. As well established in the literature, we found that the more intense the irradiation, the faster the photodegradation.

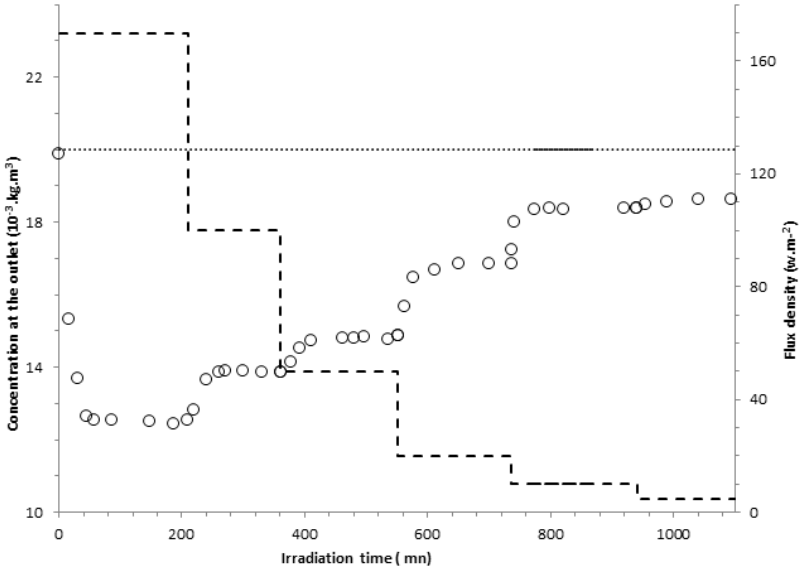

Figure 4 : Variation in the concentration at the outlet of the photoreacteur (o) for different conditions of irradiations (concentration at the inlet of the reactor of 0.02 $kg.m^{-3}$, and flow rate of 0.08 $.10^{-6}$ $m^3.s^{-1}$): flux densities equal to 170, 100, 50, 20, 10 and 5 $w.m^{-2}$ (--).

4.2.Pollutant concentration effect

In the treatment by heterogeneous photocatalysis, the influence of concentration is widely described in the literature[27, 32-33]. However, most of these studies were conducted in batch

systems. We therefore set out to assess the capacities of the photocatalytic treatment in the open reactor.

As regards the feed concentration of pollutant, it was decided to keep within the usual range of concentrations, namely 0.001–0.3 $kg.m^{-3}$. The experiments were built on the same mode, i.e. with fixed operating conditions: a flow rate of $0.08.10^{-6}$ $m^3.s^{-1}$ which corresponded to a residence time of 1 h, and a flux density of 50 $W.m^{-2}$ equivalent to that reached on a sunny day. Four feed concentrations spanning the range 0.02–0.003 $kg.m^{-3}$ were applied. The time course of the concentrations at the outlet of the photoreactor is shown in Figure 5.

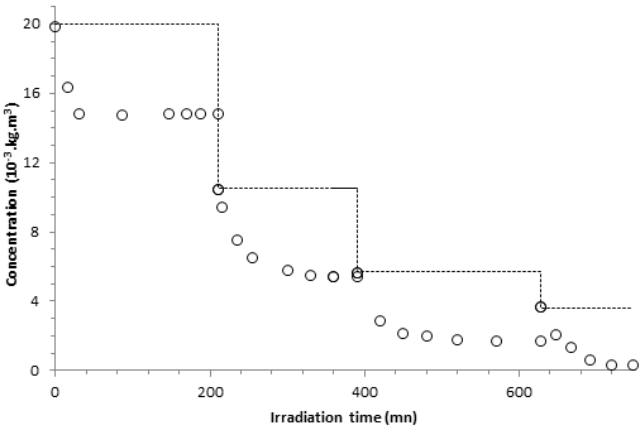

Figure 5 : Variation in the concentration at the outlet of the photoreacteur (○) for different conditions of feed (flux density of 50 $W.m^{-2}$, 0.03 and flow rate =$0.08 .10^{-6}$ $m^3.s^{-1}$): concentration at the inlet of the reactor of 0.02, 0.01, 0.006 and 0.004 $kg.m^{-3}$ (--).

Whatever the feed concentration, the concentration curves decreased until it reached a threshold after about 3 h of treatment. We note that the equilibrium concentration decreased as the input concentration decreased. In agreement with the results obtained for other categories of substance,[24, 32, 34] the photodegradation rate increased as the feed concentration increased.

4.3 Flow rate effect

Experimental data were acquired for three flow rates, 0.016, 0.08 and 0.16 ($.10^{-6}$) $m^3.s^{-1}$, while the other conditions were kept constant: feed concentration 0.020 $kg.m^{-3}$ and an applied flux density of 50 $W.m^{-2}$. The successive experiments are depicted in Figure 6. Regarding the curves showing that the concentration at the output of the reactor decreased with the flow rate, we can confirm that the photodegradation rate was a function of the residence time ($\frac{V_T}{m_v} = \tau$).

The average irradiation time ($\frac{V_r}{m_v} = \tau_{irr}$) was directly proportional to the residence time. Thus to control the pollution level at the outlet, we could act on the residence time.

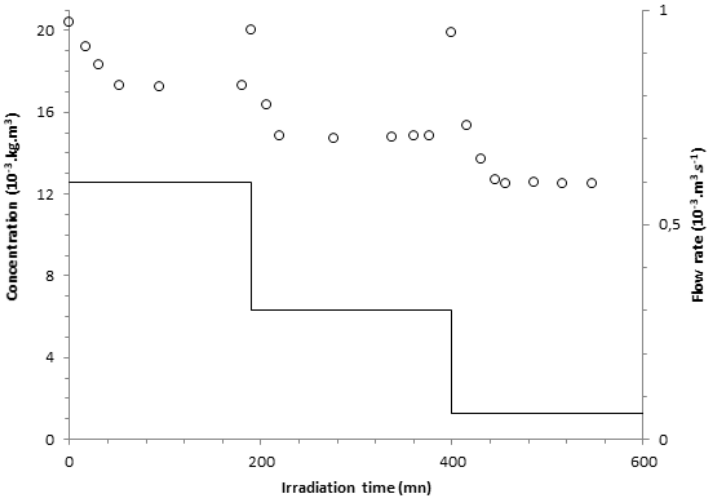

Figure 6 : Variation in the concentration at the outlet of the photoreacteur (○) for different conditions of feed (concentration at the inlet of the reactor of 0.02 kg.m^{-3} and flux density of 50 W.m^{-2}): flow rate of 0.06, 0.03 and 0.6 m^3.s^{-1} (-).

Regardless of the concentration levels at the output, the variables such as flux density, residence time and feed concentration made it possible to optimize the degradation rates. On the other hand, high concentration and/or flow rate applied to the system were unfavorable to obtaining low concentrations at the reactor outlet. Operating conditions could be modulated to obtain the best performance according to the intended application.

5. MODELLING DEGRADADTION IN THE PHOTOREACTOR

5.1. A model taking into account variable setpoints

Our aim is to model the photodegradation rates according to operating conditions. This involves both writing the material balance on the photoreactor but above all defining a kinetic law representative of photodegradation processes taking place in the photoreactor. However, there is still no analytical law representative of the mechanisms occurring during heterogeneous photocatalysis. The generally empirical expressions are based on the double dependence of photodegradation rate on pollutant concentration and on radiation flux density[5]. They make it possible to describe situations with specific conditions such flow density or concentration ranges or restricted to the fields of application, or to a given chemical

substance. For example, Emeline[32] showed that a power law with a ratio of 1 to 20 over a range of flux densities and concentrations can be used to represent the variation in degradation rate of a given molecule. However, dedicated studies seem to show that the heterogeneous degradation photoprocess proceeds in two distinct stages, i.e. one step corresponding to the transfer of matter to the solid phase (the pollutant migrates from the solution to the catalyst) and a photochemical step corresponding to compound degradation by radical attacks [33]. These two antagonistic mechanisms mean that pollutant concentration may be a limiting factor[21, 34-35]. It is possible to consider this limitation related to the transfer of compounds using Langmuir-Hinshelwood kinetics which account for effect of concentration on rate of degradation. In the literature,[5, 24, 36-37] this formalism describing the effect of pollutant concentration has been successfully validated on a number of molecules, effluents and in-effluent active substances. Here we use the formalism described by Equation (5) expressing the dependency of degradation rate on flux density and concentration irrespective of the order of the reaction.

$$\overset{\circ}{r}(C,I,t)=\left[\alpha\cdot\frac{I(t)}{1+\gamma I(t)}\right]\cdot\frac{C_o(t)}{1+\beta C_o(t)} \tag{5}$$

where $\overset{\circ}{r}$ is the speed of the photoreaction (kg.m^{-3}.s^{-1}), C_o is the concentration in the photoreactor (kg.m^{-3}) – the outlet concentration if we consider a CSTR – $I(t)$ is the light flux density at the surface of the photoreactor (W.m^{-2}), α (m^2/J) is the kinetic constant of the photoreaction, and β (m^3.kg^{-1}) and γ (m^2.W^{-1}) are adjusting numerical parameters. These two constants respectively represent a parameter modulating reaction rate with respect to concentration and a parameter modulating reaction rate with respect to irradiation[20, 25, 38]. In this expression, $I(t)$, the irradiation at the surface of the reactor, was intentionally adopted as the reference. Working with the mean volumetric irradiation conditions is easy using the ratio of the reactor surface area to the reactor volume. In the perspective of defining the degradation rates, the resolution of the differential equation expresses the variation in the concentration at the outlet of the photoreactor taking into account the operating conditions (flow rate, inlet concentration, flux density) and the reactor characteristics (volume, irradiated surface area). Hereafter, this equation will be used, based on only three parameters to be determined: α, β, and γ:

$$\frac{dC_o(t)}{dt}=\frac{1}{\tau}\cdot(C_o(t)-C_i(t))-\frac{V_r}{V_T}\cdot\left[\alpha\cdot\frac{I(t)}{1+\gamma I(t)}\right]\cdot\frac{C_o(t)}{1+\beta C_o(t)} \tag{6}$$

Table 1 summarizes the various features of the processing loop, such as the total operating volume V_T, the volume of the photo-reactor V_r, the ratio of the irradiated volume to the total volume $\frac{V_r}{V_T}$, the range of available radiation flux densities I, the range of available flow rates m_v, the corresponding residence time τ and the residence time in the irradiated cell τ_{irr}.

V_T (m^3)	V_r (m^3)	$\frac{V_r}{V_T}$ (−)
0.0002	0.00015	0.75
C_i ($kg.m^{-3}$)	Q ($10^{-6}.m^3.s^{-1}$)	I ($w.m^{-2}$)
0.001-0.02	0.06-0.16	1-170
τ (h)		τ irr (h)
0.06-0.6		0.036-0.36

Table 1 : characteristics of the photoreactor and typical setpoints applied.

5.2.Parameter determination

One of the advantages of working in an open reactor and a steady state is having direct experimental access to degradation rates. These are calculated simply and accurately from Equation (4). These rates were set under different experimental conditions, ultimately resulting in terms for irradiation levels at the reactor surface and concentrations in the reactor.

As previously for estimating residence time, the parameters in the kinetic law (Equation (5)) were found by criterion minimization. However, the process was carried out in two stages. A first step working on the tests carried out at variable concentrations, but at an identical irradiation of 50 $W.m^{-2}$ (Figure 5) gave $\beta = 1.21\ 10^3$ ($m^3.kg^{-1}$) and one value representative of the product of α and the term $I/(1 + \gamma.I)$. In a second step, the values of $\alpha = 1.46\ 10^{-4}$ $m^2.J^{-1}$ and $\gamma = 1.91\ 10^{-2}$ ($m^2.W^{-1}$) were determined for the experiments carried out at different levels of irradiation (Figure 4), keeping the previously determined value of γ.

In all cases, the selected kinetics associated with the values of the coefficients indicated above allowed an estimation in agreement with the experimental rates obtained for the various conditions of operation of the photoreactor. To validate the approach, the speed of degradation deduced from experimental data and Equation (5) are reported in Figure 7 as a function of the inlet concentration. In the range considered, the degradation rate increased significantly at low concentrations and tended to stabilize for larger values of feed concentrations.

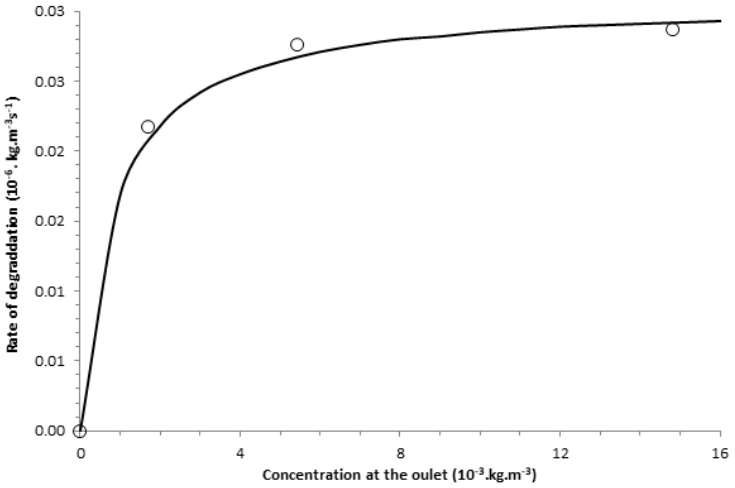

Figure 7 : Variation in the rate of MO photodegradation (○) according to the concentration at the inlet of the reactor (flux density of 50 $W.m^{-2}$, 0.03 and flow rate =0.08 $.10^{-6}$ $m^3.s^{-1}$). Rate f degradation is simulated with Eq. 5 for $\alpha = 1.46\ 10^{-4}$ $m^2.J^{-1}$, $\beta = 1.21\ 10^3$ $m^3.kg^{-1}$ and $\gamma = 1.91\ 10^{-2}$ $m^2.W^{-1}$.

These results, consistent with the literature, show that the model described by Equation (5) is closely representative of the capabilities of the photoreactor to degrade MO. We note that the parameters had been set beforehand (Tab. 1). For each applied flux density, the photodegradation rate also deduced from experimental and calculated data are reported in Figure 8 as a function of the flux density. This result, well established in the literature, shows that the more intense the irradiation, the faster the photodegradation. Although as expected the rate of degradation was increased with irradiation, saturation of the catalyst was not reached in the range of UV power from 1 to 3 suns. It can be seen that the variation of the speed as a function of the flux density can also be described with Equation (5) with determined parameters (Tab. 1).

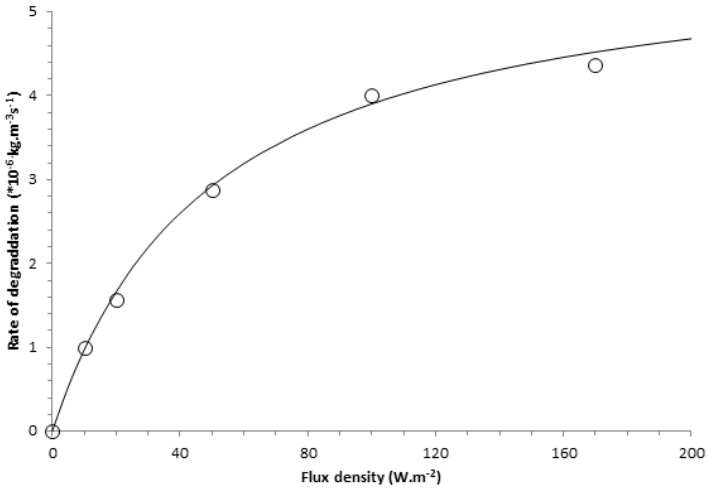

Figure 8 : Variation in the rate of MO photodegradation (○) according to the flux density (concentration at the inlet of the reactor of 0.02 kg.m^{-3}, and flow rate of 0.08 .10^{-6} m^3.s^{-1}). Rate f degradation is simulated with Eq. 5 for α =1.46 10^{-4} m^2.J^{-1}, β = 1.21 10^3 m^3.kg^{-1} and γ = 1.91 10^{-2} m^2.W^{-1}.

6. SIMULATION OF A SOLAR EXPERIMENT

Although there are already a wide range of research studies related to the photocatalytic degradation of pollutants using sunlight,[22, 39-40] almost all are designed for degradation assessment in batch operations. The scant experimentation reported on the effect of illumination cycles was conducted on gas-phase photodegradation[23]. To open up the possibility of real applications in this field, we needed to simulate the capacity of a photoreactor to treat water in dynamic mode. A dynamic mode involves operating with an open reactor under variable setpoints. Knowing that solar irradiation is an intermittent resource that depends on the local irradiation of the daily and seasonal cycles,[24, 41] the photoreactor was employed in experiments conducted under artificial illumination simulating daily variation of sunlight.

Secondly, experiments conducted in a dynamic mode are essential for testing the robustness and reliability of the kinetic model. To this end, once steps of parameter identification and validation had been completed by means of the results obtained for different operating conditions, a simulated solar irradiation experiment was carried out. These experiments were conducted under irradiation conditions corresponding to typical days in February and July at Perpignan, generated using METEONORM software. To be consistent with the conditions of the experiments, the UV irradiation conditions were determined for a surface oriented north-south and tilted at 45°. The variation in the flux density during the day

is reported in Figure 9 and 10. The experiment began early in the morning and ended late in the evening.

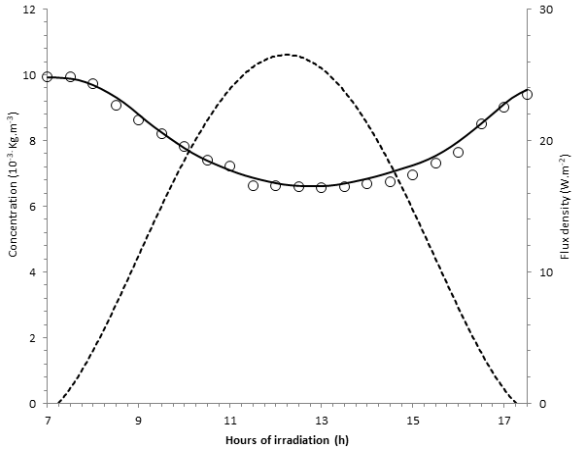

Figure 9 : Concentration evolution of MO (○) under a irradiation corresponding to a typical day of February (--). Initial conditions: concentration at the inlet of the reactor is 0.001 kg.m^{-3} and flow rate applied is 0.08 .10^{-6} m^3.s^{-1}. Results are fitted with Eq. 6 (-) for α =1.46 10^{-4} m^2.J^{-1}, β = 1.21 10^3 m^3.kg^{-1} and γ = 1.91 10^{-2} m^2.W^{-1}.

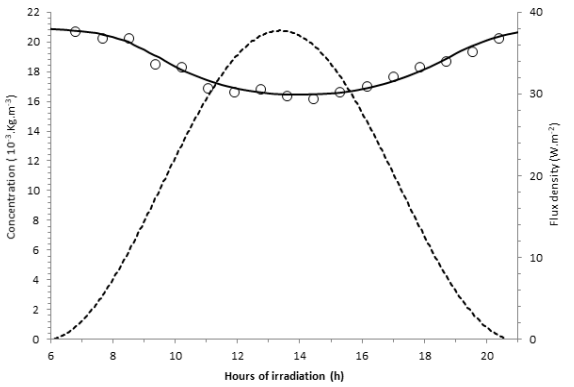

Figure 10 : Concentration evolution of MO (○) under a irradiation corresponding to a typical day of July (--). Initial conditions: concentration at the inlet of the reactor is 0.002 kg.m^{-3} and flow rate applied is 0.08 .10^{-6} m^3.s^{-1}. Results are fitted with Eq. 6 (-) for α =1.46 10^{-4} m^2.J^{-1}, β = 1.21 10^3 m^3.kg^{-1} and γ = 1.91 10^{-2} m^2.W^{-1}.

The level of the outlet concentration of the photoreactor was observed between 6:30 and 17:30 up to the level of the feeding concentration (Figure 9). As expected, the degradation of the pollutant increased as the solar irradiation increased during the morning from 0 to 27 W.m^{-2}. When the maximal conditions were reached in the middle of the day, the concentration in the reactor was 6.62 kg.m^{-3}, which corresponds to a rate of degradation of 2.1 .10^{-6} kg.m^{-3}.s^{-1}. During the second phase of the day, irradiations declined to zero flux density after 10 h of experiment. Conversely, under low irradiation conditions, degradation was reduced. At the end of the day, the concentration tended towards the concentration of feed (C = 0.0105 kg.m^{-3}). The system perfectly mirrored, with opposite sign, the time course of the flux density. We clearly see the dependence of the speed of degradation on the level of the flux density, and the process was able to adapt to external conditions. In Figure 10, the second campaign conducted on a typical July day shows similar behaviour.

To simulate the variation of the pollutant concentration, Equation (6) was solved taking into account the inlet conditions applied to the system, but especially the irradiation conditions: the irradiation setpoint of a typical February day represented by the function $I(t)$ is integrated in Equation (6). We emphasize that no supplementary adjustment of α, β and γ was done. Values previously determined for the three parameters involved in the kinetic law α = 1.46 10^{-4} m^2.J^{-1}, β = 1.21 10^3 m^3.kg^{-1} and γ = 1.91 10^{-2} m^2.W^{-1}, were used directly in the simulation. Experimental and simulated data are reported in Figure 9 and 10. The fact that the

concentration profiles from the experiments and the modelling coincided throughout the entire course of the reaction helps validate the model proposed for simulating the photoreactor. It is interesting to observe the changes in the simulated concentration with the level of irradiation. The two daily periods displayed a significant increase and decrease in the degradation kinetics corresponding to the variation in the daily irradiation.

It is noteworthy that the model, whose parameters had been identified when the photoreactor operated in a steady state, perfectly described the situation of degradation during a sunny day. This involves dynamic operation due to both the continuous feed of pollutant at the reactor input and the irradiation conditions, so the flow density is variable over time. The formalization used with Equation (5) thus seems to accurately describe the time course of the photoreactor in both steady and transient states.

CONCLUSION

In this work, we developed a flat-plate open reactor irradiated with a LED panel to study photocatalytic MO degradation in a permanent working mode. The utility of this operating mode was that we could apply varied setpoints to assess the degradation capacity of the photoreactor under conditions close to those of a real processing system. The initial conditions applied mimicked sunny conditions (flux density corresponding to the range of solar irradiation) and the residence time that of biological treatment ponds. The photoreactor subjected to different feed conditions (flow rate and concentration) and irradiation (fixed or variable flow density) showed a strong dependence of the responses on the operating conditions. The numerous experimental results yielded a representative model of the different conditions tested. With three adjustment parameters ($\alpha = 1.46\ 10^{-4}$ $m^2.J^{-1}$, $\beta = 1.21\ 10^3$ $m^3.kg^{-1}$ and $\gamma = 1.91\ 10^{-2}$ $m^2.W^{-1}$) characteristic of concentration and irradiation dependences that were set (and not adjusted) for all the tests performed, this model was robust over conditions close to those envisaged for treatment applications: irradiation range 1–170 Wm^{-2}, concentration range 0.001–0.002 $kg.m^{-3}$ and flow rate range 0.016–0.16 ($.10^{-6}$) $m^3.s^{-1}$ (corresponding to residence times of 0.06–0.6 h). The experimental results obtained in permanent and transient conditions were accurately described by the proposed formalization.

The purpose of this work was to acquire experimental data under simulated solar irradiation representative of typical days during the year (February and July were selected as an example). The model established under these dynamic conditions, with the objective of providing a dimensioning tool for the design and scale-up of solar reactors working in

dynamic mode, was validated. In took good account of the influence of UV flux density, pollutant concentration, and the discontinuous nature of sunlight irradiation.

AKNOWLEDGEMENTS

This work received European sponsorship via the FEDER funds under the " Interreg SUDOE" program (Innovec'eau SOE1/P1/F0173) and government sponsorship via the National Research Agency under the "Avenir investissements" program (ANR-10-LABX-22-01).

REFERENCES

[1] M. Salgot, M. Folch, *Current Opinion in Environmental Science & Health*, **2018**, 2, 64–74

[2] Water Framework Directive 2000/60/EC of the European Parliament and of the Council of 23 October **2000** establishing a framework for Community action in the field of water policy.

[3] T. Ternes, *Wat. Sci. & tech*, **2007**, 55, 327-332.

[4] C. Vasilis, E. Sarasidis, V. Konstantinos, V. Plakas, I. Sotiris, I. Patsios, and J. Karabelas, *Chemical Engineering Journal*, **2014**, 239, 299-311.

[5] G. Plantard and V. Goetz, *Chemical Engineering and Processing*, **2012**, 62, 129-136.

[6] M. Miguet, V. Goetz, G. Plantard and Y. Jaege, *Industrial and Engineering Chemistry Research*, **2015**, 54, 9813-9823.

[7] M. Brienza, M. Mahdi Ahmed, A. Escande, G. Plantard, L. Scrano, S. Chiron, S. Bufo and V. Goetz, *Che. En. J*, **2014**, 257, 191-199.

[8] M. Brienza, S. Mir, G. Plantard, L. Scrano, S. Chiron and V. Goetz, *ESPR*, **2018**, 3.

[9] S. Malato, J. Blanco, C. Richter, P. Fernandez, MI. Maldonado, *Solar Energy Materials & Solar Cells*, **2000**, 64, 1-14.

[10] S. Malato, J. Blanco, A.Vidal, C. Richter, *Applied Catalysis B: Environmental*, **2002**, 37, 1-15.

[11] S. Malato, J. Blanco, A. Campos, J. Caceres, C. Guillard, JM. Herrmann, AR. Fernandez-Alba, *Applied Catalysis B: Environmental*, **2003**, 42, 342-357.

[12] S. Malato, J. Blanco, MI. Maldonado, P. Fernandez-Ibanez, D. Alarcon, M. Collares, J. Farinha, J. Correia de Oliveira, *Solar Energy*, **2004**, 77, 513-524.

[13] S. Malato, P. Fernandez-Ibanez, MI. Maldonado, J. Blanco, W. Gernjak, *Catalysis Today*, **2009**, 147, 1-59.

[14] I. Mesquita, LC. Matos, F. Duarte, FJ. Maldonado-Hódar, A. Mendes, A. Madeira., *J. Hazard. Mater*, **2012**, 237, 30–37.

[15] MI. Stefan, *Fundamentals and Applications IWA publishing*, London, 2018.

[16] J. Wu, C. Lan, G. Chan, *Chemosphere*, **2009**, 2, 1308-1314.

[17] R. Andreozzi, C. Caprio, A. Insola, R. Marotta, *Catal. Today*, **1999**, 53, 51–59.

[18] ME. Leblebici, J. Ronge, JA. Martens, GD. Stefanidis, T. Van Gerven, *Chemical Engineering Journal*, **2015**, 264, 962–970

[19] J. Galvez and S. Malato, *Scientific and Cultural Organization*, **2003**.

[20] M. Kacem, G. Plantard, M. Brienza and V. Goetz, *Industrial engineering chemistry research*, **2017**, 51, 15001-15007.

[21] F. Zhang, J. Zhao, T. Shen, H. Hidaka, E. Pelizzetti, N. Serpone, *App. Cat. B: Envir*, **1998**, 15, 147-156.

[22] AR. Ricardo, R. Monteiro, C. Rodrigues-Silva, F. Lopes, A. Silva, R. Boaventura, V. Vilar, *Chemical Engineering Journal*, **2015**, 280, 409–416.

[23] H. Chen, Y. Ku, A. Irawan, *Chemosphere*, **2007**, 69, 184–190

[24] T. Janin, V. Goetz, S. Brosillon and G. Plantard, *Solar Energy*, **2013**, 87, 127-135.

[25] V. Goetz, JP. Cambon, D. Sacco and G. Plantard, *Chemical Engineering and Processing*, **2009**, 48, 532-537

[26] M. Kacem, G. Plantard, N. Wery, V. Goetz, *AICHE*, **2015**, 61, 8.

[27] JM. Herrmann, *Catalysis today*, **1999**, 53, 115-129.

[28] A. Rosset, G. Plantard, K. Djessas, Photocatalytic efficiencies of $Zn_{1-x}M_xO$ compounds synthetized with a band panel of M elements : Responses in the UV, visible and solar range., J. Environmental Chemical Engineering, 6 (2018), 7273-7283.

[29] C. Dezani, C. Calliot, G. Plantard and V. Goetz, Experimentation and modelling of the degradation capacities of a heterogeneous photocatalysis photoreactor based on the description of locals radiative transfer and kinetics, Industrial and Engineering Chemistry Research (submitted).

[30] M. Miguet, V. Goetz, G. Plantard and Y. Jaeger, *Industrial and Engineering Chemistry Research*, **2015**, 54, 9813-9823.

[31] W. Konicki, D. Sibera, E. Mijowska, Z. Lendzion-Bieluń, U. Narkiewicz, *J.Colloid Interface Sci.* **2013**, 398, 152−60.

[32] AV. Emeline, V. Ryabchuk, N. Serpone, *Journal of photochemistry and photobiology*, **2000**, 133, 89-97.

[33] C. Minero, *Catalysis Today*, **1999**, 54, 205-216.

[34] L. Lhomme, S. Brosillon, T. Wolbert, *Chemosphere*, **2008**, 70, 381-386.

[35] D. Friedmann, C. Mendive, D. Bahnemann, *Appl. Catal. B Environ*, **2010**, 99, 398–406.

[36] D. Spasianon, R. Marotta, S. Malato, P. Fernandez-Ibanez, and I. Di Somma, *Applied Catalysis B: Environmental*, **2016**, 170, 190-223.

[37] M. Ballari, R. Brandi, O. Alfano, and A. Cassano, *Chemical Engineering Journal***, 2008**, 136, 50-65.

[38] G. Plantard and V. Goetz, *Chemical of Engineering Journal***, 2014**, 52, 194-201.

[39] W. Jo, S. Shin, ES. Hwang, *Journal of Hazardous Materials*, **2011**, 191, 234–239

[40] HP. Kuo, CT. Wu, RC. Hsu, *Powder Technology*, **2009**, 195, 50–56

[41] F. Correia, V. Goetz, G. Plantard and D. Sacco, Journal of solar energy *engineering***, 2011**, 133, 1-6